arXiv:0803.2073v1 [cond-mat.mtrl-sci] 14 Mar 2008

Half Metallicity in Hybrid BCN Nanoribbons

Er-Jun Kan[1], Xiaojun Wu[2], Zhenyu Li[1], X. C. Zeng[2*], Jinlong Yang[1,*] and J. G. Hou[1]
[1]*Hefei National Laboratory for Physical Sciences at Microscale, University of Science and Technology of China, Hefei, Anhui 230026, China*
[2]*Department of Chemistry and Nebraska Center for Materials and Nanoscience, University of Nebraska-Lincoln, Lincoln, Nebraska 68588, USA*
(Dated: March 14, 2008)

We report a first-principles electronic-structure calculation on C and BN hybrid zigzag nanoribbons. We find that half-metallicity can arise in the hybrid nanoribbons even though stand-alone C or BN nanoribbon possesses a finite band gap. This unexpected half-metallicity in the hybrid nanostructures stems from a competition between the charge and spin polarizations, as well as from the π orbital hybridization between C and BN. Our results point out a possibility of making spintronic devices solely based on nanoribbons and a new way of designing metal-free half metals.

PACS numbers: 75.75.+a, 73.22.-f, 73.20.Hb

The discovery of low-dimensional carbon allotropes such as fullerenes [1] and nanotubes [2] has stimulated intensive research on metal-free magnetism, owing to their small spin-orbit coupling and long spin scattering length. Since the first report of room-temperature weak ferromagnetism in polymerized C_{60} [3], magnetism in pure carbon materials has been demonstrated by several experimental groups [4, 5, 6]. Carbon defects or adatoms are believed to be the origin for the unexpected magnetism [7, 8, 9].

A question arises that can low-dimensional carbon nanostructures exhibit half metallicity? Half metals are ideally for spintronic applications because they have one metallic spin channel and one semiconducting or insulating spin channel. Techniques for tuning electronic properties of graphene nanoribbon (GNR) have been advanced [10, 11, 12], for example, by terminating a single graphite layer in one direction. Recently, Son *et al.* [13] predicted, based on density functional theory (DFT) calculation, that zigzag edge GNRs (ZGNRs) can be converted to half metal when an external transverse electric field is applied onto the graphene layer. Our recent study using hybrid DFT confirmed their prediction[14]. However, we found that a very strong field is required to achieve half metallicity, a limitation for wide application.

In the absence of external field, ZGNRs are semiconductor with two localized electronic edge states [15, 16, 17, 18, 19]. These two ferromagnetically ordered edge states are antiferromagnetically coupled. In the presence of an external field, an electrostatic potential difference is generated between the two ZGNR edges, which causes band crossing and charge transfer between the two edge states. As a result, the ZGNRs are converted to half metal from semiconductor. Since the critical step to make half-metallic ZGNR is to break the symmetry of the two edge states, an alternative approach is to use chemical decoration. For nanoelectronic applications, the chemical approach has many advantages over the strong-field approach.

In this Letter, we present two nanostructure designs to achieve half-metallicity for carbon nanoribbons without using metal dopants. The first design is by implanting a BN row into a ZGNR. The principle of this materials design is based on the following observation: both the highest valance band (VB) and the lowest conduction band (CB) of ZGNR are mainly contributed by the two edge states which have opposite spin but are degenerate in energy. In contrast, for the zigzag BN nanoribbon, the highest VB is originated from the π orbitals of the N edge atoms, while the lowest CB is mainly localized at the B edge atoms. These results suggest that the symmetry of the ZGNR band structure near the Fermi energy can be broken by introducing a segment of BN nanoribbon.

A geometry of the newly designed hybrid C/BN nanoribbon is shown in Fig 1e, where the armchair atom rows are normal to the ribbon direction while the zigzag atom chains are in the ribbon direction. At the two edges, H atoms are added to passivate the dangling σ bonds. The hybrid ribbon structures are denoted as n-C_iBN, where i refers to the number of armchair C rows in a unit cell, and n is the width of the nanoribbon in term of the number of zigzag chains. On one edge, B is the outmost non-hydrogen atom; this edge is denoted as the B-edge. The adjacent C atoms to the B-edge are named C_B. Similarly, the C atoms adjacent to the N-edge are named C_N.

The DFT calculations were carried out using the VASP package [20]. The projector augmented wave (PAW) [21] method in Kresse-Joubert implementation [22] was used to describe the electron-ion interaction. The plane wave cut-off energy was set to 400.0 eV. The convergence thresholds for energy and force were 10^{-5} eV and 0.01 eV/Å, respectively. Perdew-Wang functional [23] known as PW91 was used in the generalized gradient approximation (GGA). In a previous study of ZGNRs, we showed that the GGA gives qualitatively the same results as hybrid density functional [14]. Here, the calculated band gaps of the pristine ZGNR and BN nanoribbon with

8 zigzag atom chains are 0.43 and 4.2 eV respectively, in good agreement with previous theoretical calculations [13, 24].

The calculated electronic structures of 8-C_iBN (i=1, 2, 3) are shown in Fig 1. The band structures of 8-C_1BN and 8-C_3BN exhibit different patterns compared to 8-C_2BN, which can be understood from the Brillouin-zone folding. When i is even, the largest gap locates at Γ point, and when i is odd the smallest gap locates at Γ point. 8-C_1BN has a nonmagnetic ground state with a small band gap of ∼0.1 eV. Both 8-C_2BN and 8-C_3BN are spin-polarized, and the latter is half metal since its valence and conductive bands overlap at the Fermi level in the spin-down channel. This half-metallicity is unexpected, considering that both C and BN zigzag nanoribbons possess a finite band gap. We further examined nanoribbons with different widths ($n = 6-14$). As shown in Fig 1d, all C_iBN (i=1, 2, 3) nanoribbons become half metal when $n \geq 12$. The critical widths are n =12, 10, and 8 for i=1, 2, and 3, respectively.

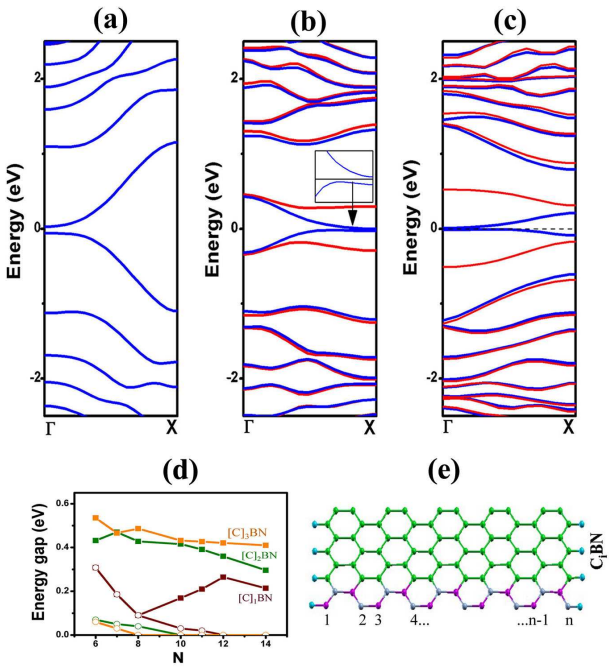

FIG. 1: Band structures for (a) C_1BN, (b) C_2BN, (c) C_3BN with 8 zigzag chains. The red (blue) lines represent the spin-up (spin down) channel. (d) The spin-resolved band gaps of n-C_iBN nanoribbons. The filled square and hollow circle denotes the spin-up and spin-down channel, respectively. (e)The atomic configuration of C_iBN ribbons. Green, pink, grey, and sapphire balls denote carbon, boron, nitrogen, and hydrogen atoms, respectively.

The calculated partial density of states (PDOS) indicates that the 8-C_1BN has no spin polarization. Near the Fermi level, the occupied states are contributed by C_N and N edge atoms, while the unoccupied states are contributed by C_B and B edge atoms. This is a charge polarized state with electron transfer from C_B to C_N. The charge polarization is clearly seen in Fig. 2a-g; the partial charge density from 0.05 eV below the Fermi level to the Fermi level is localized at the N-edge.

In pristine ZGNR, every edge C atom at the edge has only two C neighbors and thus 1/3 nonbonded extra π electron, which gives rise to the edge states and a high electron density at the Fermi level. A stablization mechanism is required to have a lower-energy ground state [17]. In the charge-polarization mechanism, the extra electron transfers completely from one edge to the other. In the spin-polarization mechanism, the C atoms at the two opposing edges have spin-opposite electrons, which lowers the on-site Coulomb interaction U between electrons with opposite spin at the same site. The spin mechanism is more favorable in energy [17]. However, the charge-polarized state can be further stabilized by an external electric field. Hence, a ZGNR can be changed from having spin polarized state to charge polarized state under external field. In either the spin or charge polarized state, a ZGNR is semiconductor. Here, the half-metallicity for ZGNR is found in the region where the two states compete with each other[14].

The charge-ordered ground state of 8-C_1BN is stablized by the mixing of π orbitals of C and BN. In C_1BN, each C_B atom is covalently bonded to a N atom, while each C_N atom is connected to a B atom. As shown in Fig. 2g, the occupied π orbital of N is much lower in energy than the unoccupied π orbital of B. The π orbitals of C locate in the middle. The interaction between the π orbitals of C_B and N results in a higher antibonding orbital. However, the electron tends to occupy the lower bonding orbital between C_N and B. Such an orbital interaction leads to electron transfer from C_B to C_N.

As the nanoribbon width (n) increases, the Coulomb interaction between the two edge states decreases, and thus the stabilization energy of the charge-polarized state also decreases. On the other hand, the on-site Coulomb interaction is a local property, and the spin-polarization energy is independent of the ribbon width [17]. Hence, the spin polarization becomes relatively more competative as the nanoribbon width increases.

As shown in Fig 2b, when the ribbon width is not wide enough (e.g., n = 10), the ribbon still has an occupied N-edge and nearly empty B-edge state. However, the spin degeneracy is already broken. The spin-up and spin-down electrons tend to occupy one of the two subsites of the honeycomb lattice, which leads to the energy of spin-down edge state higher than of the spin-up one. When n=12, the occupied spin-down state at the N-edge and the unoccupied spin-down state at the B-edge cross over in energy. The B-edge is partly occupied, which weakens the charge polarization. More importantly, in this case, the spin-down channel becomes metallic. Therefore, the competition between the spin and charge polarization leads to half-metallicty in this hybrid-ribbon

structure. As the ribbon width increases, a decrease of charge polarization (Fig. 2a-c) and an increase of spin polarization (Fig. 2d-f) can be clearly seen.

For C_iBN with $i > 1$, the π orbital hybridization only occurs between BN and its nearest neighboring C atom row. In the $i{=}\infty$ limit, the electronic structure of C_iBN will converge to that of ZGNR. For different i, we analyzed the competition between charge and spin polarization and the half-metallicity based on the spin-polarized ZGNR ground state (see Fig. 2h). In ZGNR, C atoms at the two edges are degenerate in energy but with opposite spin. When the BN row is introduced, the energy of the bonding π orbital between C_N and B is lower than that of the edge state in ZGNR. This bonding state is occupied by spin-up electrons. On the other hand, for C_B and N, both the bonding and anti-bonding states are occupied by the spin-down electrons. Hence, in C_iBN without charge polarization, the valence band maximum (VBM) stems from the anti-bonding states between N and C_B in the spin-down channel, while the conduct band minimum (CBM) is composed of the bonding states between B and C_N in the same spin channel. With the increase of the ribbon width, the ZGNR band gap is reduced, and the VBM and CBM are closer in location. Once the VB and CB overlaps at a specific point ($i{=}3$ and $n{=}8$), spin-down electron at the B-edge will transfer to N-edge. Consequently, at both edges, the spin-down channel is partially occupied, and the partial charge polarized nanoribbon becomes half metal.

Note that implantation of a BN row in carbon nanotube has been realized in the laboratory [25, 26], but not yet in ZGNR. Our first design for the hybrid C/BN nanoribbon is a highly ordered nanostructure. It may be challenging to realize this nanostructure in the laboratory but it can serve as a proof of principles for achieving metal-free half metal. For the purpose of practical (mass) production of the ZGNR-based half metal, we propose an alternative material design as illustrated in Fig. 3 (left panels). Here, a pair of B and N atoms are doped in place of two C atoms in each supercell of ZGNR (dilute substitution). The location of the substitution is arbitrary. In Fig. 3 (right pannels), we show the calcualted DOS for five typical configurations of the BN substitution, three at the edge and two in the interior of the ZGNR. It can be seen that with the exception of the symmetric substitution at the opposing edge [Fig. 3(c)], four out of five configurations exhibit spin polarization also. Some hybrid nanoribbons can be viewed as spin-selective semiconductor [e.g. in the case of Fig. 3(b)].

The most interesting case is the configuration shown in Fig. 3(e), where both B and N atoms are located in the interior of the ZGNR but not as a nearest neighbor. Appreciable DOS can be seen near the Fermi level in the spin-up channel whereas a finite band gap can be seen in the spin-down channel. The calculated band structure (left panel in Fig. 4) shows that there is a very narrow band gap in the spin-up channel (about a few tens of meV). Hence, this heterogeneous nanoribbon exibits half-metal or half semi-metal like behavior. This result suggests that half metallicity can be achieved by doping B and N atoms within the interior region of the ZGNR. The doping can be random as long as it is dilute to assure certain separation between the B and N atoms. To confirm this design, in Fig. 4 (middle and right panels), we show the calculated band structures for two additional

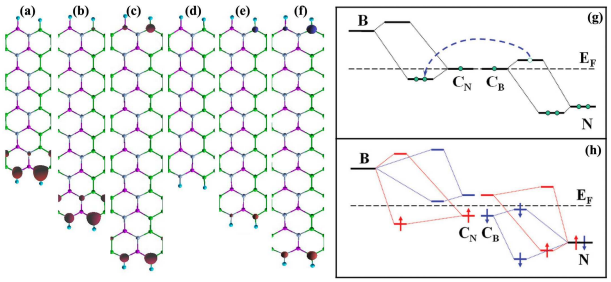

FIG. 2: The partial charge density within energy range [E_f-0.05, E_f] in eV for n-C_1BN with n equals to (a) 8, (b) 10, and (c) 12. Isovalue is 0.02 e/Å^3. Spin density of n-C_1BN with n equals to (d) 8, (e) 10, and (f) 12. (g) and (h) are schematic energy diagram for C_iBN. (g) Charge polarization caused by π electron hybridization between C and BN. The blue arrow indicates the direction of electron transfer. (h) Competition between spin and charge polarization. Spin degenerated orbitals are represented by long level lines, and spin orbitals are denoted by short level lines. Red and blue represent the spin up and spin down channel, respectively.

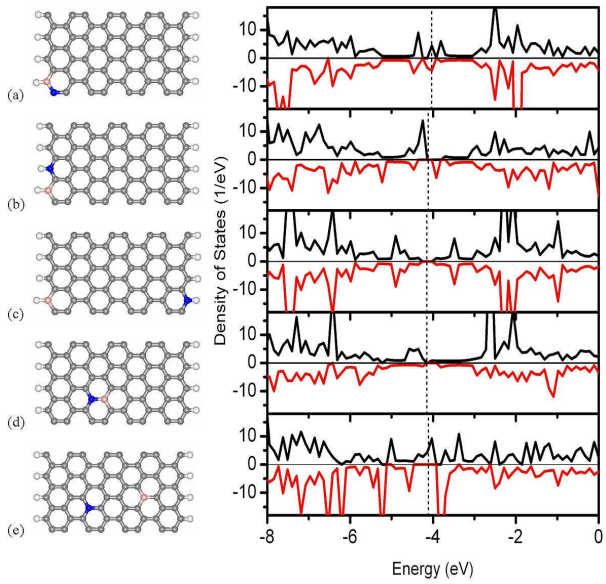

FIG. 3: (a) $\sim$ (e) Configurations and density of states of a pair of B and N atoms substituted ZGNR. Fermi level is plotted with dotted line. Grey, blue, khaki and white balls denote carbon, nitrogen, boron, and hydrogen atoms, respectively.

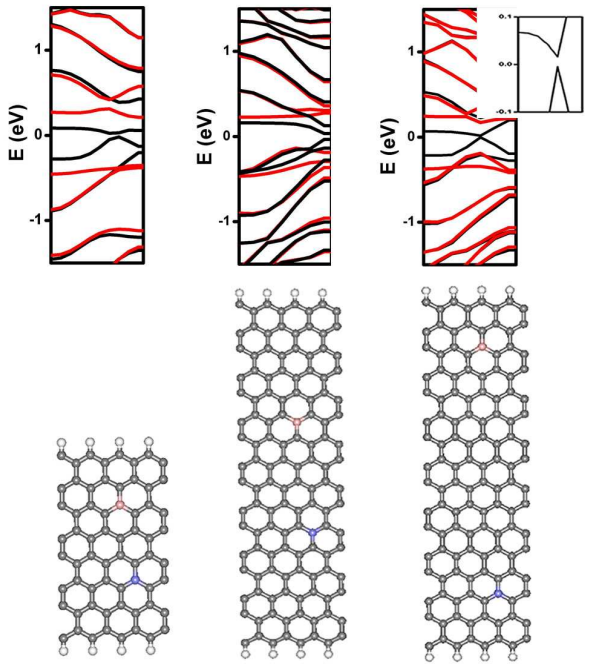

FIG. 4: Band structures of randomly doped ZGNR with different width. Red for the spin-up channel, and black for the spin-down channel.Grey, blue, khaki and white balls denote carbon, nitrogen, boron, and hydrogen atoms, respectively.

doping configruations in a wider ZGNR. Evidently, the band gap in one spin channel is narrower. This result suggests that electrons in this spin channel behave like metal (or semi-metal), especially when the the B and N atom is located near the two opposing edges, respectively (right panel in Fig. 4).

In conclusion, we have studied spin-dependent electronic properties of heterogeneous C/BN nanoribbons using density functional theory. We find that a ZGNR can be converted to half metal (or half semi-metal) either by inbedding an ordered BN row in ZGNR or by substituting B and N atoms in the interior of ZGNR. In both cases, the π orbital hybridization between C and B (or N) breaks the symmetry of the two edge states. Finally, we note that in both material designs no metal dopants are involved. This metal-free half-metallicity points to a new venue for making spintronic/electronic devices at low-cost.

This work is partially supported by the National Natural Science Foundation of China (50121202, 20533030,20628304), by National Key Basic Research Program under Grant No.2006CB922004, by the USTC-HP HPC project, and by the SCCAS and Shanghai Supercomputer Center. The UNL group is also supported by US DOE (DE-FG02-04ER46164), NSF, and the Nebraska Research Initiative.

* Corresponding author. E-mail: jlyang@ustc.edu.cn; xczeng@phase2.unl.edu

[1] H. W. Kroto, J. R. Heath, S. C. O'Brien, R. F. Curl, R. E. Smalley, Nature (London) **318**, 162 (1985).
[2] S. Iijima, Nature (London) **354**, 56 (1991).
[3] T. L. Makarova, B. Sundqvist, R. Höhne, P. Esquinazi, Y. Kopelevich, P. Scharff, V. A. Davydov, L. S. Kashevarova, and A. V. Rakhmanina, Nature (London) **413**, 716 (2001).
[4] P. Esquinazi, A. Setzer, R. Höhne, C. Semmelhack, Y. Kopelevich, D. Spemann, T. Butz, B. Kohlstrunk, and M. Lö che, Phys. Rev. B. **66**, 024429 (2002).
[5] R. A. Wood, M. H. Lewis, M. R. Lees, S. M. Bennington, M. G. Cain, and N. Kitamura, J. Phys. Condens. Matter, **14**, L385 (2002).
[6] J. M. D. Coey, M. Venkatesan, C. B. Fitzgerald, A. P. Douvalis, and I. S. Sanders, Nature (London) **420**, 156 (2002).
[7] P. O. Lehtinen, A. S. Foster, A. Ayuela, A. Krasheninnikov, K. Nordlund, and R. M. Nieminen, Phys. Rev. Lett. **91**, 017202 (2004).
[8] P. O. Lehtinen, A. S. Foster, A. Ayuela, T. T. Vehvilinen, and R. M. Nieminen, Phys. Rev. B. **69**, 155422 (2004).
[9] Y. C. Ma, P. O. Lehtinen, A. S. Foster, and R. M. Nieminen, New J. Phys. **6**, 68 (2004).
[10] K. S. Novoselov, A. K. Geim, S. V. Morozov, D. Jiang, M. I. Katsnelson, I. V. Grigorieva, S. V. Dubonos, A. A. Firsov, Nature (London), 2005, **438**,197, 2005.
[11] Y. B. Zhang, Y. W. Tan, H. L. Stormer, P. Kim, Nature (London), **438**, 201, 2005.
[12] C. Berger, Z. M. Song, X. B. Li, X. S. Wu, N. Brown, C. Naud, D. Mayou, T. B. Li, J. Hass, A. N. Marchenkov, E. H. Conrad, P. N. First, and W. A. de Heer, Science, **312**, 1191, 2006.
[13] Y.-W. Son, M. L. Cohen, S. G. Louie, Nature (London), **444**, 347, 2006.
[14] E.-j. Kan, Z. Y. Li, J. L. Yang, J. G. Hou, cond-matt: 0708.1213.
[15] K. Kusakabe and M. Maruyama, Phys. Rev. B. **67**, 092406 (2003).
[16] H. Lee, Y.-W. Son, N. Park, S. Han, and J. Yu, Phys. Rev. B. **72**, 174431 (2005).
[17] L. Pisani, J. A. Chan, B. Montanari, and N. M. Harrison, Phys. Rev. B, **75**, 064418 (2007).
[18] V. Barone, O. Hod, and G. E. Scuseria, Nano Lett. **6**, 2748 (2006).
[19] O. Hod, V. Barone, J. E. Peralta, G. E. Scuseria, Nano Lett. **7**, 2295 (2007).
[20] G. Kresse, and J. Hafner, Phys. Rev. B **47**, 558 (1993).
[21] P. E. Blochl, Phys. Rev. B **50**, 17953 (1994).
[22] G. Kresse, and D. Joubert, Phys. Rev. B **59**, 1758 (1996).
[23] J. P. Perdew, J. A. Chevary, S. H. Vosko, K. A. Jackson, M. R. Pederson, D. J. Singh, and C. Fiolhais, Phys. Rev. B **46**, 6671 (1992)
[24] J. Nakamura, T. Nitta, and A. Natori, Phys. Rev. B **72**, 205429 (2005).
[25] O. Stephan, P. M. Ajayan, C. Colliex, Ph. Redlich, J. M. Lambert, P. Bernier, and P. Lefin, Science **266**, 1683 (1994).
[26] Enouz, S.; Stephan, O.; Cochon, J.-L.; Colliex, C. Loiseau, A. *Nano Lett.* **2007**, 7, 1856.